Familial autosomal recessive bestrophinopathy: identification of a novel variant in BEST1 gene and the specific metabolomic profile

Panpan Ye
Zhejiang University
Jia Xu
Zhejiang University
Yueqiu Luo
Zhejiang University
Zhitao Su
Zhejiang University
Ke Yao (xlren@zju.edu.cn)
https://orcid.org/0000-0002-6764-7365

Research article

Keywords: Autosomal recessive bestrophinopathy; BEST1; mutation; metabolomics

Posted Date: September 25th, 2019

DOI: https://doi.org/10.21203/rs.2.14948/v1

Version of Record: A version of this preprint was published on January 22nd, 2020. See the published version at https://doi.org/10.1186/s12881-020-0951-3.

Abstract

Background Autosomal recessive bestrophinopathy (ARB) is a retinal degenerative disorder caused by BEST1 mutations with autosomal recessive inheritance. We aim to map a comprehensive genomic and metabolic profile of a consanguineous Chinese family with ARB.Methods Ophthalmic examinations were performed on affected patients with ARB. Target capture sequencing was performed to screen causative mutations in 256 known retinal disease genes and Sanger sequencing were used for verification. A UHPLC-MS/MS metabolomic analysis was performed to explore the disease-associated metabolic feature.Results Affected patients from this family are characterized by low vision, the presence of subretinal fluid, macular edema, and hyperopia with coincidental angle closure. DNA sequencing identified a novel missense mutation in BEST1 gene (chr11:61725867G>A) of the proband. Sanger sequencing further confirmed the mutation. The blood metabolic profiles were very similar among all family members probably due to the same life style, habitats and genomic background. However, ARB patients presented significant deregulation of metabolites such as Citric acid, L-Threonic acid, Eicosapentaenoic acid.Conclusions We identified a novel disease-associated variant in BEST1 gene as well as the disease-specific metabolic feature in familial ARB. The findings improved the understanding of mechanisms of ARB and provided a potential therapeutic strategy with application of metabolomics.

Background

Mutations of the BEST1 gene can cause a series of retinal degenerative diseases which are named as the “bestrophinopathies” [1]. The most common of these diseases clinically is Best vitelliform macular dystrophy (BVMD; OMIM 153700), also known as Best disease. It is characterized by the deposition of bilateral yellowish yolk-like lesions in the macula. Most BVMD is inherited in an autosomal dominant type by mutations of the BEST1 gene [1]. Recently, an allelic disease, autosomal recessive bestrophinopathy (ARB; OMIM 611809), has been firstly reported by Burgess R [2]. It is also caused by BEST1 mutation with autosomal recessive inheritance [3-5]. The clinical phenotype can be different from BVMD. The features of ARB present with multifocal yellow subretinal deposits, subretinal fluid, macular edema and hyperopia with coincidental angle closure. People with ARB demonstrate a decrease in vision during the first ten years of life.

The exact function of BEST1 gene still remains elusive, but it is speculated to act as coding for anion channel, mainly a chloride and bicarbonate channel, or a regulator of Ca^{2+} channels in retinal pigment epithelium (RPE). So far, more than 250 mutations have been explored in bestrophinopathies (http://www-huge.uni-regensburg.de/BEST1_database/) [1]. In ARB, almost half of the mutations are located between residues 312 and 315. The most common mutation for ARB is p.R15H in several families of European ethnicity and p.R255W in Chinese ethnicity [1, 6, 7]. However, the whole genomic map of ARB and the underlying mechanism are still far from completely understood.

The metabolome affects biological and physiological processes through modulation of genetic transcription and translation and interactions with environmental exposures [8]. Due to the fast

development in techniques and bioinformatics, metabolome has been used to not only identify biomarkers for diagnosis but also provide therapeutic strategy in diseases. However, the application of metabolome to retinal diseases has been limited [9]. We herein conducted a metabolomics study in a consanguineous Chinese ARB family. We aimed to explore the disease-associated genomic and metabolic feature for better understanding the etiology of ARB and providing the intervention strategy.

Methods

Clinical diagnosis

The patients were ascertained at Eye Center, Second Affiliated Hospital, School of Medicine of Zhejiang University, China. They underwent detailed ophthalmic evaluation, including best correct visual acuity (BCVA), slit-lamp bio-microscopy, dilated indirect ophthalmoscopy, anterior chamber (ultrasound biomicroscopy, UBM; SUOER UBM scan SW-3200), widefield retinal imaging (Optos 200Tx, Marlborough, MA, USA), optical coherence tomography (OCT) (Heidelberg HRT II, Heidelberg, Germany) and fundus fluorescein angiography (FFA) (Heidelberg HRT II, Heidelberg, Germany) examinations. All research involved in this study adhered to the tenets of the Declaration of Helsinki and was approved by the Institutional Review Board of Second Affiliated Hospital of Zhejiang University. Informed written consents were obtained from all participating individuals for this study.

DNA library preparation and target sequencing

Genomic DNA of the proband and available family members was extracted from peripheral blood. A pre-capture library was prepared by using Kapa LTP library prep kit and then was captured on a custom capture panel (Agilent Sureselect) which containing 256 known retinal disease genes. The enriched DNA library was sequenced on Illumina Xten Analyzers for 150 cycles per read to generate paired-end reads. An average of 172.82X in target region was achieved, and 97.86 % of the target region was covered by 10x.

Bioinformatics analysis and Sanger sequencing

After the sequencing step, Raw reads were aligned to the human genome reference (hg19) using the Burrows-Wheeler Aligner. Single-nucleotide variants (SNVs) and InDels (Insertions and Deletions) were called by Atlas-SNP2 and Atlas-Indel, respectively. SNVs and InDels were filtered against the ExAC, gnomAD, HGVD, CHARGE, 1000 Genome, UK10K databases and the internal database of Clinbytes Inc, with a allele frequency cutoff of 0.5% and 0.1% for recessive and dominant variants, respectively. Variants were annotated using Annotate Variation (ANNOVAR). The variant was validated by PCR and Sanger sequencing. PCR primer sets were designed via Primer3 and products were sequenced on an ABI 3700XL Genetic Analyzer.

UHPLC-MS/MS metabolomics analysis

Patients peripheral blood were collected and plasma were prepared for LC-MS/MS analysis, which were performed using a Vanqiush UHPLC system (Thermo Fisher) coupled with an Orbitrap Q Exactive HF-X mass spectrometer (Thermo Fisher) operating in the data-dependent acquisition mode. The eluents for the positive and negative polarity mode were eluent A (0.1% FA in Water) plus eluent B (Methanol) and eluent A (5 mM ammonium acetate, pH 9.0) plus eluent B (Methanol), respectively. The solvent gradient was set as follows: 2% B, 1.5 min; 2-100% B, 12.0 min; 100% B, 14.0 min□100-2% B, 14.1 min□2% B, 16 min. Q Exactive HF-X mass spectrometer was operated in positive/negative polarity mode with spray voltage of 3.2 kV, capillary temperature of 320°C, sheath gas flow rate of 35 arb and aux gas flow rate of 10 arb. The raw data files were processed using the Compound Discoverer 3.0 (CD 3.0, Thermo Fisher) to perform peak alignment, peak picking, and quantitation for each metabolite. The normalized data was used to predict the molecular formula based on additive ions, molecular ion peaks and fragment ions. And then peaks were matched with the mzCloud (https://www.mzcloud.org/) and ChemSpider (http://www.chemspider.com/) database to obtain the accurate qualitative and relative quantitative results.

Results

Clinical features

It is a consanguineous Chinese family with Han Chinese ancestry. The proband is a 34-year-old woman with progressive vision loss for over 20 years. Her BCVA was 0.15 on right eye and 0.1 on left eye. Colour funduscopy (CF) showed overall normal (**Fig. 1a**). Fundus autofluorescence (FAF) image showed annular hyperfluorescence around the posterior pole (**Fig. 1b**). OCT results revealed cystoid macular edema with subretinal fluid (**Fig. 1c**). The proband has an affected younger sister aged 32, with 20 years of progressive vision loss. Her BCVA was 0.1 in both eyes. Her clinical findings in CF, FAF and OCT were similar with the proband. In addition, she had a shallower anterior chamber depth and UBM showed half of the anterior chamber angles were closed (**Fig. 1d**). FFA revealed mild fluorescence leakage beneath macula (**Fig. 1e**). The proband also has an affected elder sister aged 36, with over 20 years of progressive vision loss. Both of her eyes underwent vitrectomy for retinal detachment and her visual acuity in both eyes was counting fingers.

Genetic mapping

We performed target capture sequencing of known retinal disease genes on the proband to identify possible mutation. A homozygous variation in gene BEST1 was detected in 256 gene coding regions associated with retinal diseases in peripheral blood of the subjects. The variant in BEST1 gene

(chr11:61725867G>A) was confirmed in the proband. According to the splicing form of the proband (uc010rlu.1), the novel mutation BEST1 c.646G>A(p.V216I) locates in exon 7. This is a missense mutation resulting in a replacement of Valine by Isoleucine at amio acid position 216. All available family members were Sanger sequenced for the segregation analysis (**Fig. 2**). The results of family separation and analysis showed that the proband, her fifth sister and younger sister are carrying the homozygous variation, and all of them have low vision. The mother and the son of the proband and the son of her younger sister carry the heterozygosity, and the clinical phenotype of the three is normal..

Metabolomic profiles

We performed a metabolomic exploration to evaluate the potential inherited metabolic disorders, which could be diagnostic or therapeutic targets. Samples were divided into 3 groups (A/A, n = 2; A/G, n = 2; G/G, n = 3) according to the genotype in chr11:61725867 loci. The distribution of metabolites is shown in **Fig. 3a**. We observed a very similar blood metabolite profiles in this family, which may due to the same life style, habitats and genomic background. Using a criteria ($P < 0.05$, VIP > 1.0), there were 2.0-2.6% (fold change > 1.2) and 1.2-2.0% (fold change > 2.0) metabolites significantly differential expressed between two groups (**Table 1**). Compared with their 3 wild-type sisters (G/G), the proband and her fifth sister, both of whom were A/A homozygous variant type, showed significantly down-regulated Citric acid (fold change > 20), Flurothyl, L-Threonic acid, Eicosapentaenoic acid (EPA), etc. and up-regulated Hydrogen sulphate, Manidipine, 2,4-Dichlorobenzoyl-CoA, Acetate, etc. (**Fig. 3b**). Compared with their parents (A/G), they (A/A) also presented significantly down-regulated Citric acid and Flurothyl, and up-regulated Hydrogen sulphate and 2,4-Dichlorobenzoyl-CoA. The enrichment analyses of differential expressed metabolites indicated a centre role of Citric acid in enriched metabolic pathways (**Fig. 3c**). Therefore, we recommend lemonade, which riches in Citric acid and vitamin C, for the ARB patient. After three months, the proband presented improved clinical phenotype. OCT showed decreased macular edema compared with the presence of initial visit (**Fig. S1**), although no significant change was found in FAF.

Discussion

We identified a novel homozygous variation in BEST1 gene in the consanguineous family. This is an missense mutation and predicted to be deleterious. The frequency of this mutation is higher than autosomal recessive mode of BEST1 mutations as reported by the public database (http://www-huge.uni-regensburg.de/BEST1_database/home.php?select_db=BEST1). In this family, three affected patients with the mutation c.646G>A(p.V216I) are homozygous and have similar clinical phenotype. Three other members carrying the heterozygosity don't show any phenotype of ARB. The finding further proved the inheritance pattern of ARB is autosomal recessive. Therefore, among the betrophinopathies, ARB is presumed to be a retinal disease with a "null" phenotype for Best1 [2, 10].

The mutations of BEST1 can cause various clinical features [1]. To date, over 250 mutations have been explored through the BEST1 gene and the most mutations occurred in the N-terminal part, which is highly

conserved among various species [11]. However, the mutation spectrum of Chinese population may be different from patients of other ethnicity. In a Chinese cohort with 20 ARB patients, more than 1/3 mutations (9/22) in BEST1 gene were located in exon 7-11, which encode the C-terminal half of the protein [7]. The other mutations were mainly clustered in the first trans-membrane domain and the intra-cellular regions [7]. In functional prediction analysis, the majority of disease-causing variants were missense mutations [7], which was in consistent with our results. Although the disease-associated nonsense and frameshift mutations predict a truncated and thus likely inactive protein, the molecular mechanism underlying the effect of missense mutation on protein function and the pathology of disease has not been well elucidated yet. Uggenti et al [12] showed that ARB-associated BEST1 protein were degradation via the ubiquitin-proteasome pathway using a stably transfected polarised epithelial cell model. Milenkovic et al [13] further proved that the ARB-associated missense mutations triggered a strong and fast protein degradation process in the endoplasmic reticulum, thereby favouring a decreased stoichiometry of mutant versus normal BEST1 subunits in the assembly of the homo-pentameric BEST1 chloride channel.

In this study, we used a metabolome strategy to investigate the BEST1 mutation-caused disease. The family members presented very similar metabolic profiles probably due to the same life style, environment, dietary, habitats, and genomic background. We assumed that the deregulation of metabolites may be due to or at least linked with the autosomal recessive disorder. We found a remarkably insufficiency of metabolites such as Citric acid, L-Threonic acid and EPA in the blood of patients as compared to their sisters. Citric acid or citrate is a key component of the TCA cycle, serves as a pivotal regulator of intermediary energy metabolism, and a chelator for divalent cations like Ca^{2+}, Mg^{2+}, and Zn^{2+} [14]. It is uptook by human RPE cells as a preferred nutrient [15] and its buffer is widely used in the *in vivo* retina experiments. L-threonate acid is a metabolite of ascorbate (vitamin C), which is highly concentrated in the retina and plays an important role in physiological function and protects RPE from oxidant injury [16, 17]. A systemic review including 6150 participants demonstrated that antioxidant vitamin could slow the progression of age-related macular degeneration [18]. In addition, the biological importance of Omega-3 fatty acids (EPA and Docosahexaenoic Acid) in the development of retina is well established. A recent *in vivo* study showed that EPA supplementation could reduce lipofuscin granules and slow the progression of retinal degeneration [19]. Therefore, lack of these metabolites indicated a defective nutrition of human body including retina. According to the results from metabolome, we recommended a dietary Citric acid and vitamin C supplementation in the ARB patient. We pleasantly found an alleviation of macular edema after a short-term metabolic therapy. The results encouraged the patients to receive longer and more comprehensive nutrient supplement (e.g., Omega-3 fatty acid) to meet the metabolic needs and even correct the genetic disease.

Conclusions

We provided a new insight on the genomic and metabolic profiling of the pathological changes in familial ARB. Normalizing the patient's metabolism by nutritional supplement may provide a potential therapeutic

strategy for bestrophinopathy, which is currently an untreatable set of diseases.

Abbreviations

BVMD, Best vitelliform macular dystrophy

ARB, autosomal recessive bestrophinopathy

RPE, retinal pigment epithelium

BCVA, best correct visual acuity

OCT, optical coherence tomography

FFA, fundus fluorescein angiography

SNV, Single-nucleotide variants

InDels, Insertions and Deletions

CF, Colour funduscopy

FAF, Fundus autofluorescence

EPA, Eicosapentaenoic acid

Declarations

ACKNOWLEDGMENTS

None.

AUTHORS' CONTRIBUTIONS

PY, JX and YL colllected samples, performed experiments and analyzed the data. PY and ZS performed clinical examination. PY designed the study and wrote the manuscript. KY supervised the study. All authors read and approved the final manuscript.

FUNDING

This study was supported by Zhejiang Natural Science Foundation Project of China (No. LY18H120001) and National Natural Youth Science Foundation Project of China (No. 31500795).

AVAILABILITY OF DATA AND MATERIALS

The datasets used during the current study are available from the corresponding author on reasonable request.

ETHICS APPROVAL AND CONSENT TO PARTICIPATE

This study was approved by the Institutional Review Board of Second Affiliated Hospital of Zhejiang University and in accordance with the 1964 Helsinki Declaration. Informed written consent was obtained for all participants.

CONSENT FOR PUBLICATION

Written informed consents were obtained from all individuals.

COMPETING INTERESTS

The authors declare that they have no competing interests.

CONTRIBUTOR INFORMATION

Panpan Ye, Email: yepanpan@zju.edu.cn

Jaixu, Email: xujia522@zju.edu.cn

Yueqiu Luo, Email: yueqiu_luo@zju.edu.cn

Zhitao Su, Email: suzhitao@zju.edu.cn

Ke Yao, Email: xlren@zju.edu.cn

References

1. Johnson AA, Guziewicz KE, Lee CJ, Kalathur RC, Pulido JS, Marmorstein LY, Marmorstein AD: **Bestrophin 1 and retinal disease**. *Prog Retin Eye Res* 2017, **58**:45-69.
2. Burgess R, Millar ID, Leroy BP, Urquhart JE, Fearon IM, De Baere E, Brown PD, Robson AG, Wright GA, Kestelyn P *et al*: **Biallelic mutation of BEST1 causes a distinct retinopathy in humans**. *Am J Hum Genet* 2008, **82**(1):19-31.
3. Kinnick TR, Mullins RF, Dev S, Leys M, Mackey DA, Kay CN, Lam BL, Fishman GA, Traboulsi E, Iezzi R *et al*: **Autosomal recessive vitelliform macular dystrophy in a large cohort of vitelliform macular dystrophy patients**. *Retina* 2011, **31**(3):581-595.
4. Iannaccone A, Kerr NC, Kinnick TR, Calzada JI, Stone EM: **Autosomal recessive best vitelliform macular dystrophy: report of a family and management of early-onset neovascular complications**. *Arch Ophthalmol* 2011, **129**(2):211-217.
5. Lee CS, Jun I, Choi SI, Lee JH, Lee MG, Lee SC, Kim EK: **A Novel BEST1 Mutation in Autosomal Recessive Bestrophinopathy**. *Invest Ophthalmol Vis Sci* 2015, **56**(13):8141-8150.
6. Boon CJ, van den Born LI, Visser L, Keunen JE, Bergen AA, Booij JC, Riemslag FC, Florijn RJ, van Schooneveld MJ: **Autosomal recessive bestrophinopathy: differential diagnosis and treatment options**. *Ophthalmology* 2013, **120**(4):809-820.
7. Tian L, Sun T, Xu K, Zhang X, Peng X, Li Y: **Screening of BEST1 Gene in a Chinese Cohort With Best Vitelliform Macular Dystrophy or Autosomal Recessive Bestrophinopathy**. *Invest Ophthalmol Vis Sci* 2017, **58**(9):3366-3375.
8. Levine B, Kroemer G: **Biological Functions of Autophagy Genes: A Disease Perspective**. *Cell* 2019, **176**(1-2):11-42.
9. Lains I, Gantner M, Murinello S, Lasky-Su JA, Miller JW, Friedlander M, Husain D: **Metabolomics in the study of retinal health and disease**. *Prog Retin Eye Res* 2018.
10. Pomares E, Bures-Jelstrup A, Ruiz-Nogales S, Corcostegui B, Gonzalez-Duarte R, Navarro R: **Nonsense-mediated decay as the molecular cause for autosomal recessive bestrophinopathy in two unrelated families**. *Invest Ophthalmol Vis Sci* 2012, **53**(1):532-537.
11. Boon CJ, Klevering BJ, Leroy BP, Hoyng CB, Keunen JE, den Hollander AI: **The spectrum of ocular phenotypes caused by mutations in the BEST1 gene**. *Prog Retin Eye Res* 2009, **28**(3):187-205.
12. Uggenti C, Briant K, Streit AK, Thomson S, Koay YH, Baines RA, Swanton E, Manson FD: **Restoration of mutant bestrophin-1 expression, localisation and function in a polarised epithelial cell model**. *Dis Model Mech* 2016, **9**(11):1317-1328.
13. Milenkovic A, Milenkovic VM, Wetzel CH, Weber BHF: **BEST1 protein stability and degradation pathways differ between autosomal dominant Best disease and autosomal recessive bestrophinopathy accounting for the distinct retinal phenotypes**. *Hum Mol Genet* 2018, **27**(9):1630-1641.
14. Westergaard N, Waagepetersen HS, Belhage B, Schousboe A: **Citrate, a Ubiquitous Key Metabolite with Regulatory Function in the CNS**. *Neurochem Res* 2017, **42**(6):1583-1588.

15. Chao JR, Knight K, Engel AL, Jankowski C, Wang Y, Manson MA, Gu H, Djukovic D, Raftery D, Hurley JB *et al*: **Human retinal pigment epithelial cells prefer proline as a nutrient and transport metabolic intermediates to the retinal side**. *J Biol Chem* 2017, **292**(31):12895-12905.
16. Domith I, Socodato R, Portugal CC, Munis AF, Duarte-Silva AT, Paes-de-Carvalho R: **Vitamin C modulates glutamate transport and NMDA receptor function in the retina**. *J Neurochem* 2018, **144**(4):408-420.
17. Wei W, Li L, Zhang Y, Geriletu, Yang J, Xing Y: **Vitamin C protected human retinal pigmented epithelium from oxidant injury depending on regulating SIRT1**. *ScientificWorldJournal* 2014, **2014**:750634.
18. Evans JR, Lawrenson JG: **Antioxidant vitamin and mineral supplements for slowing the progression of age-related macular degeneration**. *Cochrane Database Syst Rev* 2012, **11**:CD000254.
19. Prokopiou E, Kolovos P, Kalogerou M, Neokleous A, Nicolaou O, Sokratous K, Kyriacou K, Georgiou T: **Omega-3 Fatty Acids Supplementation: Therapeutic Potential in a Mouse Model of Stargardt Disease**. *Invest Ophthalmol Vis Sci* 2018, **59**(7):2757-2767.

Tables

Table 1 The number of significantly differential expressed metabolites (DEM) ($P < 0.05$, VIP > 1.0)

Comparison	Total metabolites (n)	DEM (n)	Up-regulated DEM (n)	Down-regulated DEM (n)
Fold change > 1.2				
A_A.vs.G_G_pos	990	16	8	8
A_G.vs.G_G_pos	990	24	17	7
A_A.vs.A_G_pos	990	18	14	4
A_A.vs.G_G_neg	670	25	3	22
A_G.vs.G_G_neg	670	19	6	13
A_A.vs.A_G_neg	670	14	4	10
Fold change > 2.0				
A_A.vs.G_G_pos	990	10	5	5
A_G.vs.G_G_pos	990	15	11	4
A_A.vs.A_G_pos	990	9	5	4
A_A.vs.G_G_neg	670	23	1	22
A_G.vs.G_G_neg	670	5	3	2
A_A.vs.A_G_neg	670	12	3	9

Figures

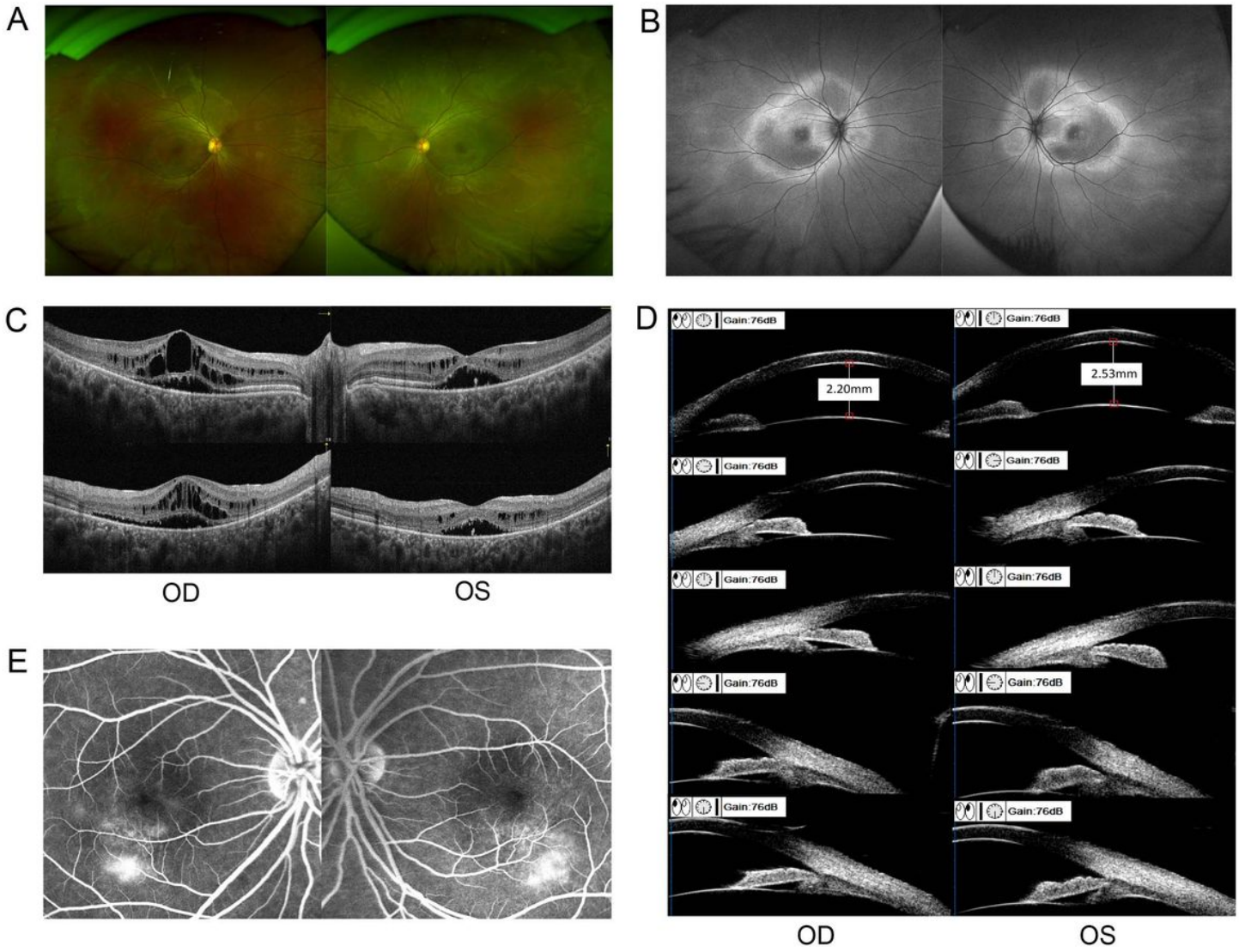

Figure 1

The clinical features of ARB patients in the family. a Colour funduscopy (CF) of the proband was overall normal. b Fundus autofluorescence (FAF) image of the proband showed annular hyperfluorescence around the posterior pole. c OCT results of the proband revealed bilateral cystoid macular edema with subretinal fluid. d The affected younger sister's ultrasound biomicroscopy (UBM) results showed a shallower anterior chamber depth and half of the anterior chamber angles were closed. e The affected younger sister's fundus fluorescence angiography (FFA) revealed mild fluorescence leakage beneath the macula.

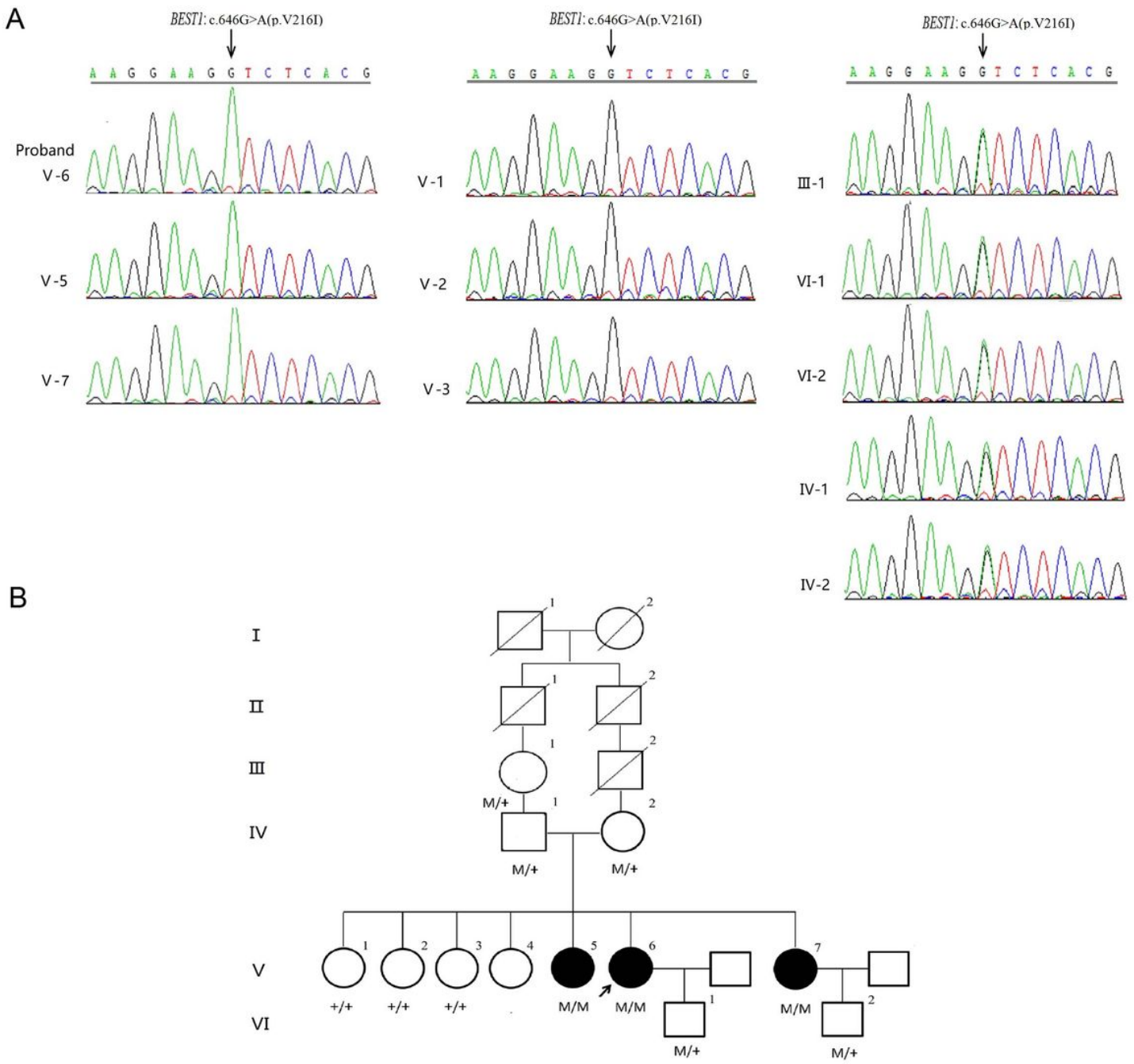

Figure 2

A novel autosomal recessive mutation in BEST1 gene (chr11:61725867G>A) was identified in the family. a The results of family separation and analysis showed that the proband (V6), her fifth sister (V5) and younger sister (V7) carry the homozygous variation. The grandmother (III-1), father (IV1) , mother (IV2) and son (VI1) of the proband, her forth sister (V4) and the son (VI2) of her younger sister carry the heterozygosity. The first sister (V1), second sister (V2) and third sister (V3) of the proband carry the wild-type gene. b Pedigree. Square symbols denote males; circular symbols denote females; solid symbols indicate affected; open symbols indicate unaffected; slashed symbols indicate deceased; an arrow below the symbol indicates the proband; + indicates wild-type.

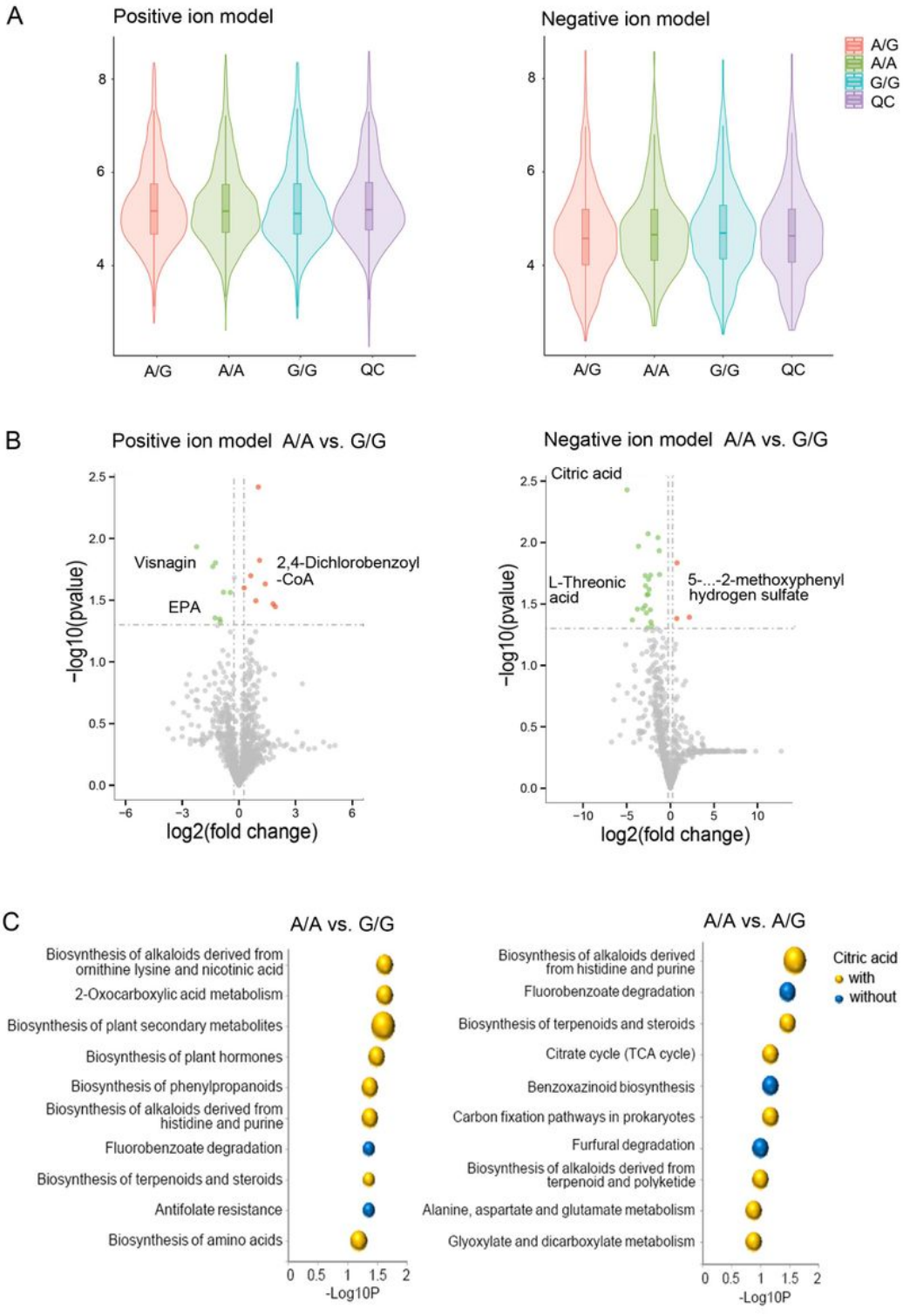

Figure 3

The metabolic profile of ARB patients. a The distribution of metabolites in the whole family. b The significantly differential expressed metabolites (fold change > 1.2, P < 0.05). (c) KEGG einrichment analysis of differential expressed metabolites between ARB patients (A/A, n = 2) and their wild-type sisters (G/G, n = 3). The size of bubble represents the number of genes in each pathway.

Supplementary Files

This is a list of supplementary files associated with this preprint. Click to download.

- Supplementaldata.doc